CHAPTER IV
CRUSTACEAN BIOMIMETIC STRUCTURED CHITOSAN - CLAY OLIGO/POLYESTER NANOCOMPOSITE

Abstract

Multicomponent nanocomposite of chitosan-clay-oligoester was proposed. In the first step, chitosan-clay nanocomposite was prepared by mixing chitosan adepate into the suspension of Na-montmorillonite. The intercalation of chitosan in clay was qualitatively analyzed by wide angle X-ray diffraction (WAXD) and the amount of chitosan adepate was determined by thermogravimetry analysis (TGA). In the second step, ethylene glycol was reacted directly with the suspension of chitosan-clay nanocomposite to achieve the esterification with diacid molecules in clay as shown by Fourier transform infrared spectroscopy (FTIR). The present work shows the possibility to form chitosan with oligo/polyester chains intercalated in clay layer which is biomimetic to the crustacean shell where chitosan, protein, cuticle, and inorganic contents all exist in the layer.

Keywords: Multicomponent nanocomposite, Oligo/polyester, Chitosan nanocomposite, Chitosan-clay nanocomposite, Biomimetic nanocomposite, Chitin-chitosan, Sodium montmorillonite

Introduction

Composite material is a macroscopic combination of two or more materials aligned to each other. Recently, the understanding of surface interaction has led to the strategies to achieve the homogeneous hybrid in the nanometer level for nanocomposite (Zhang and Gonsalves (1995)). Among nanocomposite, montmorillonite is widely applied as a main component due to its favorable structure of nanometer layer (Ruiz-Hitzky *et al.*, 2002).

At present, various nanocomposites have been developed to achieve the miscible organic-organic and/or organic-inorganic systems with the unique physical and chemical properties (Pinnavaia *et al.*, 1996). Some nanocomposites are now commercially available in the market, such as a high oxygen barrier food packaging film, NOVAMID® by Mitsubishi Engineering Plastics (www.m-ep.co.jp/mep-en/index.htm).

However, it is important to note that the original nanocomposites are from natural systems, such as bone, muscle, etc. Crustacean shells are good examples of nanocomposites with the multi-layer and components of chitin-chitosan, protein, cuticle, and inorganic minerals (Scheme I) (Berman *et al.*, 1988). It is also known that the layer structures of chitin-chitosan and protein are hardened by the function of calcium and magnesium interpenetrated in between the layers.

Considering the supra-structure of crustacean shells and nanocomposites, we pay our attention to develop an artificial one by mimicking the natural structure of those shells at molecular level. One of the most important requirements is the multicomponent of inorganic hybridized with two or more polymers co-existed in the nanocomposite. Previously, we succeeded in preparing chitosan-carboxylate salt intercalated in sodium montmorillonite. The present work, thus, focuses on the formation of polymer chain in the chitosan-clay nanocomposite. Here, the key point is that chitosan-clay nanocomposite has to be produced with monomer in the clay layer. The polymerization in clay layer is an approach for polymer intercalation co-existed with chitosan in the clay layer.

Experimental Section

Materials. Chitosan (Mv = 7 x 10^6) with a degree of deacetylation (%DD) of 85 was supplied from the SEAFRESH (Lab) Company Limited, Bangkok, Thailand. Acetic acid, hydrochloric acid and ethanol were purchased from Carlo Erba Regenti, Italy. Sodium-montmorillonite was the product of Southern Clay Product. Inc., USA. Sodium hydroxide was from Labscan Co., Inc., Thailand. Adipic acid, and ethylene glycol were obtained from Fluka Chemika, Switzerland. All chemicals were used without further purification.

Procedures. Qualitative and quantitative FTIR were obtained from a Bruker Equinox 55/S with 32 scans at a resolution of 4 cm^{-1}. A frequency range of 4000-400 cm^{-1} was observed using a deuterated triglycinesulfate detector (DTGS) with a specific detectivity, D*, of $1x10^9$ $cm.Hz^{1/2}$ w^{-1}. A Dupont thermal gravimetric analyzer was applied under air flow with a rate of 20 mL/min and heating rate of 10°C/min from room temperature to 900°C. X-ray diffraction patterns were obtained from a Rigaku RINT 2000, using CuK_α (λ=0.154 nm) with Ni filter as an X-ray source and scanning 2θ for 2°-90° at 40 kV, 30 mA.

Preparation of chitosan-clay with polyester. Chitosan-clay obtained from adipic acid solution in the weight ratio of chitosan: clay = 20:1 (see preparation of chitosan-clay nanocomposites) was stirred in 1 N hydrochloric acid (25 mL) at 50°C for 1 h. Ethylene glycol 0.4 g (7 mmol) was added to chitosan suspension and the mixture was stirred at 150°C under nitrogen for 5 h. The suspension was concentrated under vacuum and washed with methanol for several times and dried in vacuo to obtained brownish product. The characterizations were achieved by FTIR, TGA and WAXD.

Results and Discussion

Chitosan-Dicarboxylate Clay Nanocomposite Formation

WAXD technique is applied to clarify the changes in packing structure as a result from chitosan and clay interaction. In general, Na^+- montmorillonite shows d-spacing of about 12Å. Figure 1 shows the XRD pattern of chitosan-clay nanocomposite in various types of carboxylic solution (Figure 3(b)-(d)) comparing

with pure Na^+- montmorillonite (Figure 3(a)). When the carbon chain of carboxylic acid increased, the d-spacing increased. Figure 1 implies two important issues for discussion. The first is that chitosan might be intercalated effectively in clay to form nanocomposites. The second is that carboxylic acid molecules might be intercalated together with chitosan chains, as a result, the longer the chain length of carboxylic acid, the greater the d-spacing of clay.

As it is known that the interaction at molecular level between polymer chains might induce changes in vibrational modes observed by FTIR, the present work applied this technique to verify how chitosan interacted with clay. Figure 2 shows a series of chitosan patterns after treating with Na^+-montmorillonite in various dicarboxylic acid solutions (Figure 2(b)-(d)). Na^+- montmorillonite gives vibrational band of the silicate as follows; ν_{OH} for Al, Mg(OH) at 3635 cm^{-1}, and ν_{SiO} of Si-O-Si ~ 1050 cm^{-1}. There are major peaks of saccharide unit, i.e., ν_{CO} of C-O-C ~ 1075 cm^{-1}, pyranose ring ~ 890 cm^{-1}; and ν_{OH} ~ 3356 cm^{-1}, which overlap with the broad peak of the silicate around 1050 cm^{-1}. However, the peak at 1560 cm^{-1} is useful to confirm the existence of chitosan as it corresponds to the deformation vibration of the protonated amine group in chitosan. The result implied that the amino group of chitosan was in the protonated form and contributed to the electrostatic interaction between amine and negatively charged silicate on clay surface. Moreover, there is a new peak at 1700 cm^{-1}. This referred to the ν_{CO} stretching band of carboxylic acid. It is important to note that in the case of chitosan in adipic acid solution, there is a new peak at 1720 $cm^{-1}$for carboxylated ions. The result is relevant to that of Magarita *et al.* (2003) who concluded that a double layer of chitosan associated by carboxylate ion might be formed in clay layer.

TGA was applied to determine the amount of dicaboxylic acid in clay layer. Figure 3 demonstrates the degradation of a series of Na^+-montmorillonite after treating with chitosan in various dicarboxylic acids when the feed ratio of chitosan solution to Na^+-montmorillonite was fixed at the ratio of 2:1 (chitosan:clay). It is known that chitosan and dicarboxylic acid show the degradation temperature between 200°C and 400°C (Figure 4(e)) under the air atmosphere whereas clay gives the long range of degradation from 100°C to 600°C due to its moisture contents and

some inorganic salts. All nanocomposites show the degradation step from 200°C to 400°C referring to the weight loss of chitosan and dicarboxylic acid content in clay. Considering the weight loss from 200°C to 400°C for clay nanocomposite prepared from chitosan adipic acid solution, the amount of chitosan-adipate introduced into clay was found to be more than 25 wt% (Figure 4(d)).

Esterification of Chitosan-Adipate Clay Nanocomposite

As chitosan is successfully introduced into clay layer together with adipic acid, the esterification by adding a certain amount of ethylene glycol into the system was carried out. In this case, the successful reaction will not only give us the chitosan-clay oligo/polyester nanocomposite, but also confirm us indirectly that the intercalated chitosan in clay is in the form of chitosan adipate. Esterification is an appropriate model reaction as the result can be identified easily from the ester peak appearing separately from those of chitosan-clay nanocomposite. Figure 4 shows the FTIR spectra of the chitosan-clay with several carboxylic acids after esterification with ethylene glycol. Here, chitosan-clay obtained from acetic acid was also esterified with ethylene glycol to confirm the ester chain formation. In the case of chitosan-clay with monocarboxylic aicd, the FTIR spectrum shows the similar peak pattern to the one before esterification. However, in the cases of chitosan-clay obtained from dicarboxylic acid such as malonic acid, succinic acid, adipic acid, and sebacic acid, there is a new peak at 1730 cm^{-1} implying the successful esterification.

TGA was applied to follow the weight lost in the range of 400°C to 600°C referring to oligo/polyester degradation. Figure 5 shows the degradation of pure ester and chitosan-clay nanocomposite obtained from malonic acid, succinic acid, adipic acid, and sebacic acid after esterification with ethylene glycol. All types of nanocomposite obtained show the degradation step from 200°C to 400°C which refers to the weight loss of chitosan-adipate, while the step during 600°C and 800°C refers to the weight loss of inorganic content in clay. Figure 5(e) shows a new range of degradation temperature around 400°C to 600°C which might be due to the weight loss of oligo/polyester. In the cases of esterification of chitosan-clay obtained from malonic, succinic and sebacic acid systems, the average oligo/polyester content was

found to be 5 wt%. The one from adipic acid system gave significant intercalation amount of oligo/polyester of 10 wt%. The results implied that the interaction of chitosan with dicarboxylic acid and clay might be an electrostatic one under the $HOO\text{-}R\text{-}COO^{-}\text{-}NH_3^{+}$ groups of chitosan-dicarboxylate to allow the esterification with diol molecules. We speculate that esterification might occur in the layer of chitosan-clay nanocomposites between free carboxylic group of the dicarboxylic acid and the hydroxyl group of ethylene glycol as shown in Scheme II. It is important to determine the molecular weight of the ester produced in the chitosan-clay nanocomposite, the extraction process is in our future work.

WAXD technique is applied to clarify the changes in packing structure as a result from esterification in chitosan-clay nanocomposite. Figure 6(c) shows that the d-spacing of chitosan clay nanocomposite in adipic solution after esterification with ethylene glycol shifted to lower angle whereas the broad peak appeared around 20° 2θ and 30° 2θ. Comparing the result with chitosan-clay nanocomposite obtained from adipic acid (Figure 6(b)) where no broad peak was observed, we conclude that intercalation of oligo/polyester in chitosan-clay layer was a success. Figure 6(d) shows that in the case chitosan-clay obtained from acetic acid, the esterification might not be achieved as shown in its WAXD pattern which is similar to that of the starting compound (Figure 6(b)).

Conclusions

The chitosan-clay prepared by mixing chitosan in dicarboxylic acid solution was found to give nanocomposite with dicarboxylic acid molecules existed in the layer. The interaction between chitosan and clay might involve the electrostatic species of $HOO\text{-}R\text{-}COO^{-}\text{-}NH_3^{+}$ as illustrated in Scheme II. As chitosan-clay nanocomposite includes the dicarboxlic acid molecules, the esterification with acid was successful. The nanocomposite of chitosan-clay and oligo/polyester was confirmed from the peak at 1730 cm^{-1} (COOR) and the 4.7° 2θ with the broad peak at 20° 2θ as observed by FTIR and WAXD, respectively. Although we need to clarify the molecular weight of the ester species formed in chitosan-clay nanocomposite in

our future work, the present work demonstrates the successful preparation of multi-component nanocomposite of chitosan-clay polyester.

Acknowledgements. The authors wish to thank Seafresh Chitosan (Lab) Company Limited, Bangkok, Thailand for chitosan material. S.C. and N.S. acknowledge the support from The Petroleum and Petrochemical College, Chulalongkorn University, Bangkok, Thailand and The Petroleum and Petrochemical Technology Consortium, Thailand.

References

1. Zhang, S., and Gonsalves, K.E. Synthesis of $CaCO_3$-chitosan composite via biomimetic processing. *Journal of Applied Polymer Science*. **1995**, 56, 687-695.
2. Ruiz-Hitzky, E., Letaief, S., and Prevot, V. Novel organic-inorganic mesophases : self-templating synthesis and intratubular swelling. *Advanced Materials*. **2002**, 14, 436-443.
3. Pinnavaia, T. J., Lan, T., Wang, Z., Shi H., and Kaviratna, P.D. Clay-reinforced epoxy nanocomposites: synthesis, properties, and mechanism of formation. *Journal of the American Chemical Society Symposium Series*. **1996**, 17, 250-261.
4. Berman, A., Addadi, L., and Weiner, S. Interactions of sea-urchin skeletron macromolecules with growing calcite crystals-a study of intracrystalline proteins. *Nature*. **1988**, 331, 546-8.

Scheme I

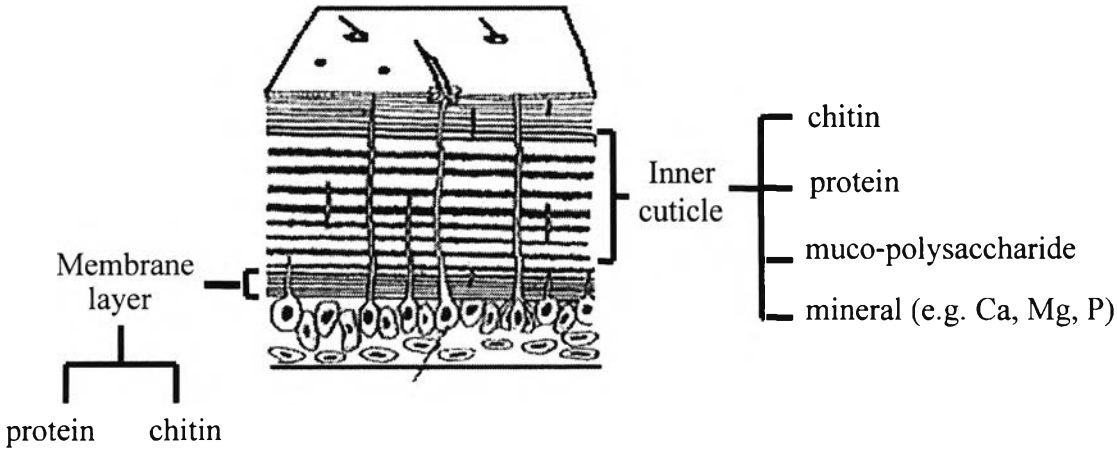
Membrane layer
protein
chitin
Inner cuticle
chitin
protein
muco-polysaccharide
mineral (e.g. Ca, Mg, P)

Scheme II

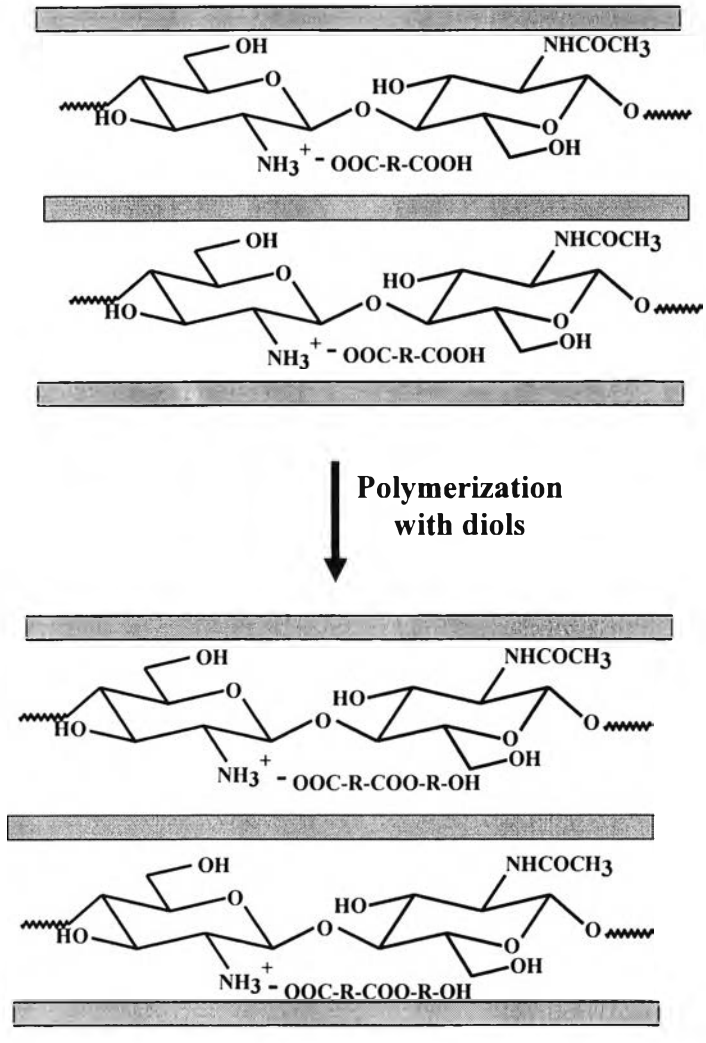
OH
NHCOCH3
HO
O
NH3+ - OOC-R-COOH
Polymerization
with diols
OOC-R-COO-R-OH

Figure Captions

Figure 1. XRD patterns of the starting Na^+- montmorillonite (a) and nanocomposites in acetic acid (b), malonic acid (c), and adipic acid (d).

Figure 2. FTIR spectra of the starting Na^+- montmorillonite (a), and nanocomposites in acetic acid (b), malonic acid (c), and adipic acid (d).

Figure 3. TG curves of Na^+- montmorillonite (a), and nanocomposites in acetic acid (b), malonic acid (c), adipic acid (d), and chitosan (e).

Figure 4. FTIR spectra of the starting Na^+- montmorillonite (a) and nanocomposites after esterification with ethylene glycol in the cases of, formic acid (b), acetic acid (c), malonic acid (d), succinic acid (e), adipic acid (f), and sebacic acid (g).

Figure 5. Degradation of chitosan-clay nanocomposite after esterification with ethylene glycol in the cases of, malonic acid (a), succinic acid (b), sebacic acid (c), adipic acid (d) and pure ester (e).

Figure 6. XRD patterns of the starting Na^+- montmorillonite (a), nanocomposites in adipic acid (b), and nanocomposites after esterification with ethylene glycol in the cases of, adipic acid (c), and acetic acid (d).

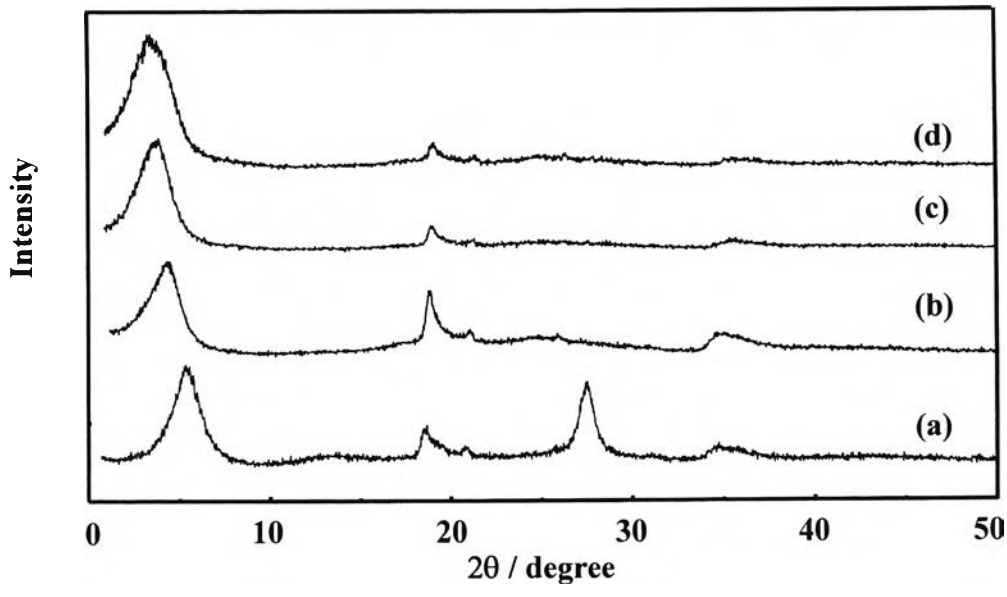

Figure 1.

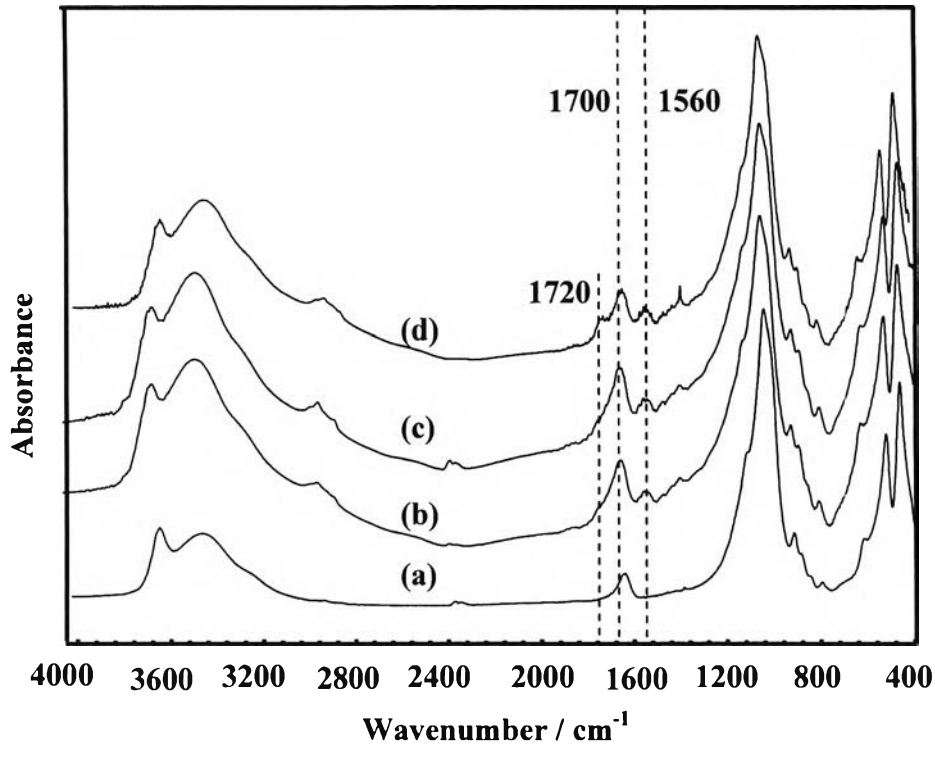
1700
1560
1720
(d)
(c)
(b)
(a)
Absorbance
4000
3600
3200
2800
2400
2000
1600
1200
800
400
Wavenumber / cm-1

Figure 2.

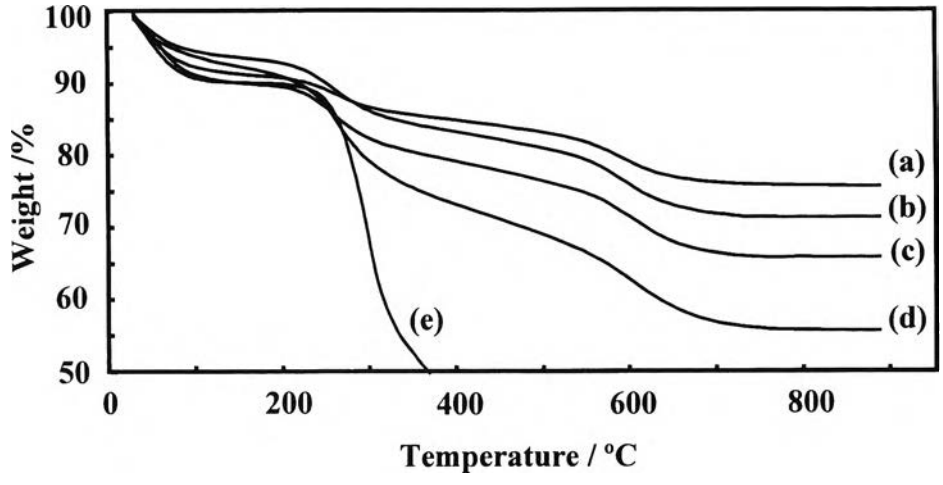

Figure 3.

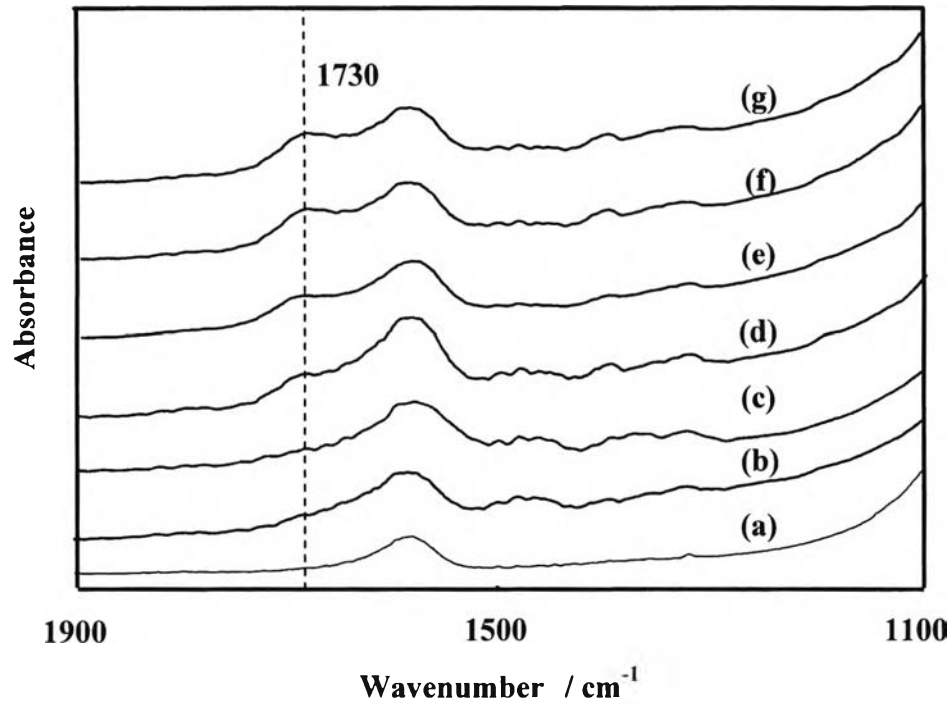

Figure 4.

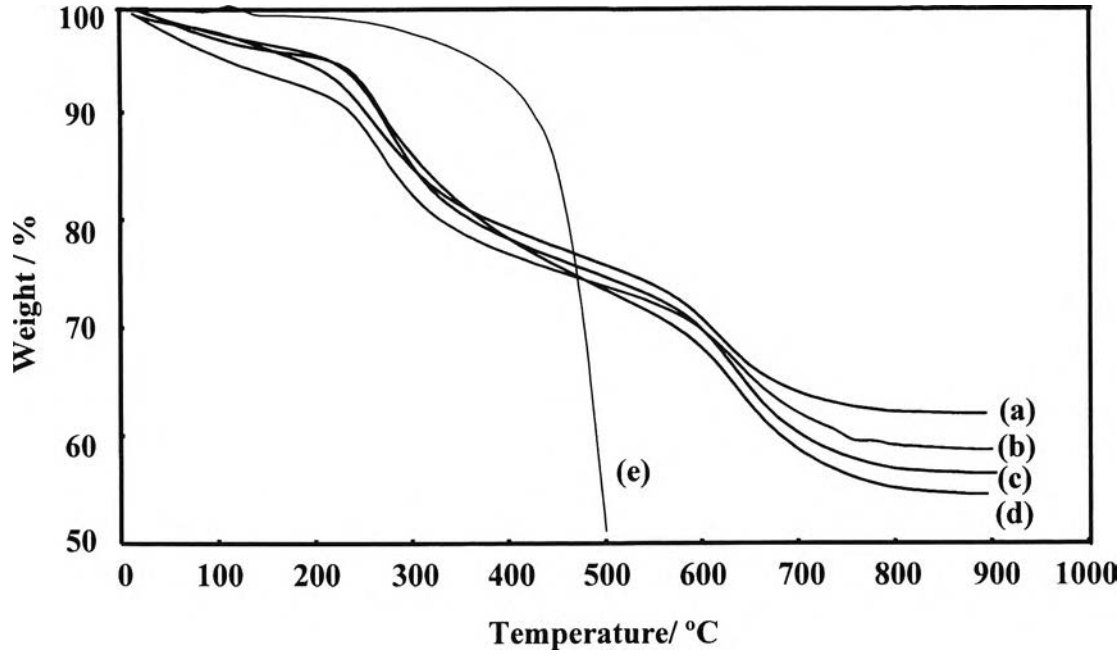
100
90
80
70
60
50
Weight / %
0
100
200
300
400
500
600
700
800
900
1000
Temperature/ °C
(a)
(b)
(c)
(d)
(e)

Figure 5.

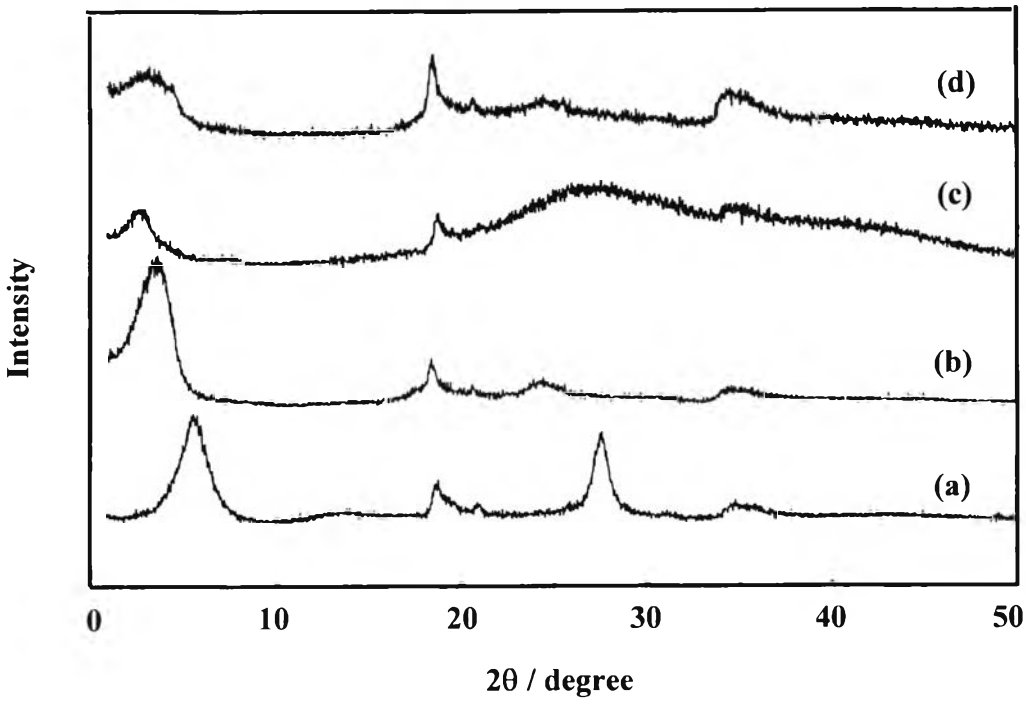

Figure 6.